in Proc. IST Mobile & Wireless Telecomm. Summit 2002, Thessaloniki (Greece), 17-19 June 2002, pp. 503–507.

Spatial and Space-Time Algorithms for Synchronisation in the Downlink of the UMTS FDD and TDD Modes

K. Kopsa[1], J.-M. Chaufray[2,3], P. Loubaton[2], F. Pipon[3], G. Matz[1], H. Artés[1], and F. Hlawatsch[1]

[1]Institute of Communications and Radio-Frequency Engineering, Vienna University of Technology
Gusshausstrasse 25/389, A-1040 Wien, Austria
phone: +43 1 58801 38983, fax: +43 1 58801 38999, email: Klaus.Kopsa@nt.tuwien.ac.at

[2]Laboratoire Système de Communication, Université de Marne-la-Vallée
5 Bd Descartes, Cité Descartes, 77454 Marne la Vallée Cedex, France
email: chaufray,loubaton@univ-mlv.fr

[3]Département Traitement du Signal, Thales Communications
66, rue du Fossé Blanc, 92231 Gennevilliers, France
email: Francois.Pipon@fr.thalesgroup.com

ABSTRACT

This paper presents methods for synchronisation in the downlink of the FDD and TDD modes of a UMTS system. Space-time processing based on multiple receive antennas is used to suppress co-channel interference caused by other base stations. We develop a detection-based synchronisation procedure exploiting the structure of the respective UMTS mode, for which we present two alternative detection algorithms. Simulation results using various propagation environments indicate the good performance of our synchronisation methods in the presence of strong co-channel interference.

I. INTRODUCTION

As third generation systems for mobile communications are starting to be deployed, network operators will require accurate measurement tools to assess the interference situation present. In the framework of the European IST project ANTIUM, we develop signal processing algorithms that allow to analyse the strength and origin of interfering signals. These algorithms attempt to demodulate the broadcast channels (BCHs) of all surrounding base stations of a UMTS network and extract the cell IDs (cf. [1] for the GSM case). Using this knowledge, it is possible to quantify how different base stations contribute to the total interference, thereby allowing network operators to adjust their network accordingly. An important prerequisite for demodulation of the BCHs is synchronisation. In this paper, we present spatial and space-time methods for synchronisation in the downlink of both modes of a UMTS system and assess their performance.

The paper is organised as follows. In Section II, we describe two detection-based synchronisation algorithms which are then used in the FDD- and TDD-specific synchronisation procedures discussed in Section III. The performance of these synchronisation procedures is finally assessed in Section IV.

II. SPACE-TIME SYNCHRONISATION ALGORITHMS

Since both UMTS modes (FDD and TDD) provide synchronisation channels containing a known primary synchronisation sequence (cf. Section III), we can use a detection approach to obtain synchronisation. The aim of such a method is to compute a decision statistic $c(n)$ for every possible time instant n. This detection statistic is processed in a subsequent stage to decide whether or not a synchronisation sequence is present at time n.

A. *Spatial Detector*

The first detector [2, 3] uses the simplifying assumption of a one-tap channel described by the single $M \times 1$ vector $\mathbf{h}$, where M is the number of antenna elements. The problem of detecting the presence of the primary synchronisation code at time n can then be formulated as the following hypothesis testing problem:

- Hypothesis H_0 (absence of synchronisation code):
  $\mathbf{x}(n+k) = \mathbf{w}(n+k)$, for $k = 0,\ldots,N-1$;
- Hypothesis H_1 (presence of synchronisation code):
  $\mathbf{x}(n+k) = \mathbf{h}\,d(k) + \mathbf{w}(n+k)$, for $k = 0,\ldots,N-1$.

Here, $\mathbf{x}(n)$ is the received signal vector, $d(k)$ is the reference sequence (synchronisation code) of length N, and $\mathbf{w}(n)$ summarises all interference from other base stations and noise. We assume that $\mathbf{w}(n)$ is Gaussian and spatially correlated with covariance matrix $\mathbf{R}$ but temporally white. Since $\mathbf{R}$ and $\mathbf{h}$ are unknown, we have to solve a composite hypothesis testing problem. In the generalised likelihood ratio test (GLRT) approach [4], we replace the unknown quantities by their conditional maximum-likelihood (ML) estimates and obtain the generalised likelihood ratio of the two hypotheses at the given time instant n as

$$L(n) = \frac{(\det \hat{\mathbf{R}}_0)^N \exp\{-Q_1(\mathbf{x})\}}{(\det \hat{\mathbf{R}}_1)^N \exp\{-Q_0(\mathbf{x})\}}, \qquad (1)$$

with

$$Q_0(\mathbf{x}) \triangleq \sum_{k=0}^{N-1} \mathbf{x}(n+k)^H \hat{\mathbf{R}}_0^{-1} \mathbf{x}(n+k),$$

$$Q_1(\mathbf{x}) \triangleq \sum_{k=0}^{N-1} \left[\mathbf{x}(n+k) - \hat{\mathbf{h}}\,d(k)\right]^H \hat{\mathbf{R}}_1^{-1} \left[\mathbf{x}(n+k) - \hat{\mathbf{h}}\,d(k)\right].$$

Here, $\hat{\mathbf{R}}_0$ and $\hat{\mathbf{R}}_1$ are the conditional ML estimates of $\mathbf{R}$ under hypothesis H_0 and H_1, respectively, and $\hat{\mathbf{h}}$ is the ML

estimate of $\mathbf{h}$. These estimates can be shown to be given by

$$\begin{aligned}\hat{\mathbf{R}}_0 &= \hat{\mathbf{R}}_{\mathbf{xx}}(n)\,,\\ \hat{\mathbf{R}}_1 &= \hat{\mathbf{R}}_{\mathbf{xx}}(n) - \frac{N}{\|d\|^2}\,\hat{\mathbf{r}}_{\mathbf{x}d}(n)\,\hat{\mathbf{r}}_{\mathbf{x}d}^H(n)\,,\\ \hat{\mathbf{h}} &= \frac{N}{\|d\|^2}\,\hat{\mathbf{r}}_{\mathbf{x}d}(n)\,, \end{aligned} \tag{2}$$

where $\|d\|^2 = \sum_{k=0}^{N-1} |d(k)|^2$ and

$$\hat{\mathbf{R}}_{\mathbf{xx}}(n) = \frac{1}{N}\sum_{k=0}^{N-1} \mathbf{x}(n+k)\,\mathbf{x}^H(n+k)\,, \tag{3}$$

$$\hat{\mathbf{r}}_{\mathbf{x}d}(n) = \frac{1}{N}\sum_{k=0}^{N-1} \mathbf{x}(n+k)\,d^*(k)\,. \tag{4}$$

After some calculations, the (logarithm of the) generalised likelihood ratio in (1) is obtained as

$$c(n) = \frac{1}{\|d\|^2}\,\hat{\mathbf{r}}_{\mathbf{x}d}^H(n)\,\hat{\mathbf{R}}_{\mathbf{xx}}^{-1}(n)\,\hat{\mathbf{r}}_{\mathbf{x}d}(n)\,. \tag{5}$$

Note that $c(n)$ involves the received signal $\mathbf{x}(n)$ within the interval $[n, n+N-1]$.

The expression (5) can be rewritten as

$$c(n) = \frac{1}{\|d\|^2}\sum_{k=0}^{N-1} z(n+k)\,d^*(k),$$

where the scalar $z(n)$ is the output of the spatial filter $\mathbf{g}(n) = \hat{\mathbf{R}}_{\mathbf{xx}}^{-1}(n)\,\hat{\mathbf{r}}_{\mathbf{x}d}(n)$ that is matched to the estimated channel vector $\hat{\mathbf{h}}$ in (2), i.e., $z(n+k) = \mathbf{g}^H(n)\,\mathbf{x}(n+k)$. Thus, $c(n)$ can be interpreted as the correlation of the filtered sequence $z(n)$ with the synchronisation code.

B. *Heuristic Space-Time Detector*

Multipath propagation was not considered by the spatial detector (5). A simple *ad hoc* method for taking into account the temporal interference caused by multipath propagation is based on stacking successive samples of the received signal vector $\mathbf{x}(n)$ into the vector

$$\tilde{\mathbf{x}}(n) \triangleq \begin{bmatrix} \mathbf{x}(n) \\ \mathbf{x}(n+1) \\ \vdots \\ \mathbf{x}(n+T-1) \end{bmatrix},$$

where T is the length of the temporal window considered. Formally substituting $\tilde{\mathbf{x}}(n)$ for $\mathbf{x}(n)$ in (5) then yields the detection statistic

$$c(n) = \frac{1}{\|d\|^2}\,\hat{\mathbf{r}}_{\tilde{\mathbf{x}}d}^H(n)\,\hat{\mathbf{R}}_{\tilde{\mathbf{x}}\tilde{\mathbf{x}}}^{-1}(n)\,\hat{\mathbf{r}}_{\tilde{\mathbf{x}}d}(n)\,,$$

where $\hat{\mathbf{R}}_{\tilde{\mathbf{x}}\tilde{\mathbf{x}}}(n)$ and $\hat{\mathbf{r}}_{\tilde{\mathbf{x}}d}(n)$ are given by (3) and (4) with $\mathbf{x}(n)$ replaced by $\tilde{\mathbf{x}}(n)$. This detection statistic is "heuristic" as it does not correspond to a GLRT with respect to the stacked signal vector $\tilde{\mathbf{x}}(n)$. Nevertheless, it can again be interpreted as a correlation of the synchronisation code with the output of a matched filter. This filter is given by $\tilde{\mathbf{g}}(n) = \hat{\mathbf{R}}_{\tilde{\mathbf{x}}\tilde{\mathbf{x}}}^{-1}(n)\,\hat{\mathbf{r}}_{\tilde{\mathbf{x}}d}(n)$.

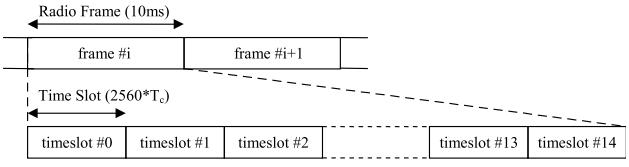

Figure 1. *Physical channel signal format [5, 6].*

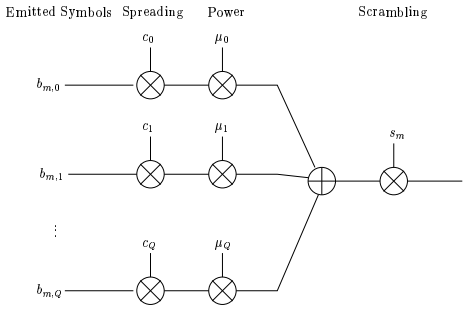

Figure 2. *Structure of the UMTS downlink.*

III. SYNCHRONISATION IN THE DOWNLINK OF UMTS

We first give a brief overview of the basic structure and parameters of the transmitted UMTS signals for both modes and then describe the structure of the physical channels that can be used for synchronisation purposes [5, 6]. We recall that the chip period is the same for all the channels, and corresponds to a duration of 0.26 ms. A slot consists of 2560 chips (0.67 ms), while a 10 ms frame consists of 15 slots (see Fig. 1).

Fig. 2 shows how the signal to be transmitted by the current base station is generated. To each logical channel a spreading factor and a spreading code are associated. The spreading code is a ± 1 sequence whose length is equal to the spreading factor. Each symbol to be transmitted is multiplied by the spreading code, thus producing a first chip rate sequence. The spreading codes allocated to the users of the same cell are orthogonal in order to improve the performance of the symbol detection algorithms.

In order to mitigate the interference generated by other base stations, this sequence is then multiplied by the so-called primary scrambling code, which is a cell-specific QPSK sequence of period 38400 chips (10 ms, i.e. one frame) for FDD and of period 16 chips for TDD. This primary scrambling code also identifies the current cell. Indeed, there are 512 different primary scrambling codes in an UMTS FDD network, and each of them is allocated to a different cell. In order to facilitate the scrambling code identification by a mobile station, the set of all scrambling codes is made of 64 groups, each of them having 8 elements.

The chip sequences associated to the various channels are added up, and in TDD a cell-specific midamble and a guard period are included in the slots. The resulting sequence is pulse-shaped and transmitted by the base station.

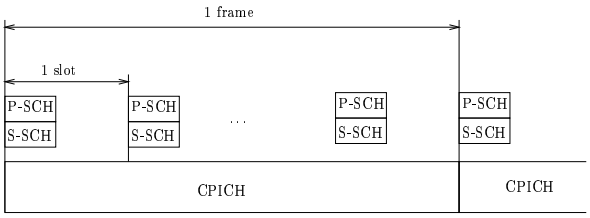

Figure 3. *Control channels in FDD.*

A. *FDD Synchronisation*

The channels relevant to synchronisation are the *primary synchronisation channel*, the *secondary synchronisation channel*, and the *common pilot channel* (see Fig. 3). The sequence transmitted by the primary synchronisation channel (P-SCH) is called the *primary synchronisation code*. It is transmitted in the first 256 chips of each slot. This code, which is not spread nor scrambled, is the same for all the cells of the network. It allows the mobile station to detect the most powerful base station in its proximity. As the various base stations of an UMTS FDD network are not synchronised, they transmit their P-SCH in a desynchronised way.

The secondary synchronisation channel is a periodic sequence of 15 codes called *secondary synchronisation codes*. These codes are transmitted in the first 256 chips of each slot; they identify the group to which the primary scrambling code of the cell belongs. This sequence is repeated in each frame. Like the primary synchronisation channel, this channel is not spread nor scrambled. There are 64 different secondary synchronisation sequences (each of them identifying the scrambling group) composed with an alphabet of 16 secondary synchronisation codes.

The chip sequence corresponding to the common pilot channel is obtained by spreading the constant symbol sequence $1+j$ by the scrambling code of the cell under consideration, the spreading factor being equal to 256. In other words the chip sequence is equal to the primary scrambling code up to the constant multiplicative factor $1+j$. The common pilot channel can thus be used in order to identify the cell, as well as to estimate the channel between the transmitter and the receiver.

Synchronisation Procedure. The detection and identification procedure described in the standard (cf. [5]) is carried out in the following three steps.

Detection of the primary synchronisation code. This allows to detect the most powerful stations and to achieve slot synchronisation with each of them. The decision statistic $c(n)$ (spatial or space-time, see Section II) is computed and compared to a threshold at each time n. Each n for which $c(n)$ is greater than the threshold is considered as a possible position of the primary synchronisation code transmitted by a base station. The threshold has to be chosen in order to achieve an acceptable false alarm rate (a false alarm occurs when $c(n)$ is greater than the threshold although the primary synchronisation code is not received at this moment) while providing a satisfactory probability of detection.

Detection of the secondary synchronisation code. The same algorithms can be applied, except that the secondary synchronisation code is used as a reference sequence. However, as the first detection step has already been performed, we just have to compare, at each position detected in the first step, the values of $c(n)$ associated to each of the 16 possible secondary synchronisation codes. Then, recombining these values, we obtain the secondary synchronisation code and its cyclic shift. The detected sequence identifies the group to which the primary scrambling code of the station belongs; the shift provides the frame synchronisation.

Detection of the scrambling code. The third step of the synchronisation procedure consists in checking the scrambling code of the detected base station. The spatial detector or the space-time detector can be used, with the synchronisation code replaced by the chip sequences corresponding to the 8 possible scrambling codes of the detected group. This last step is very reliable because, in contrast to the two synchronisation codes, the length of the scrambling code is very large. Therefore, the detection of the scrambling code can be used to confirm the detection of the synchronisation codes. For this, the maximum value of the scrambling code detection statistics is compared to a threshold. If this maximum value is greater than the threshold, the detection of the respective base station is validated; as a result, the corresponding scrambling code is identified. If the maximum value is lower than the threshold, the 8 possible scrambling codes are rejected and the detection is considered as a false alarm of the first step. This validation procedure allows to select a rather high false alarm probability at the first step of the synchronisation procedure while achieving a satisfactory overall performance.

B. *TDD Synchronisation*

The synchronisation channel (SCH) used by TDD is shown in Fig. 4. It consists of a primary and three secondary code sequences, each 256 chips long (cf. [6]). The three secondary synchronisation codes are modulated with one QPSK symbol each that bears information on the scrambling code and midamble used by the cell and on the value of the time offset $t_{\text{offset},n}$ (see Fig. 4).

TDD base stations are synchronised and therefore all SCHs are transmitted in the same time slot. The different time offsets $t_{\text{offset},n}$ prevent the SCHs of different base

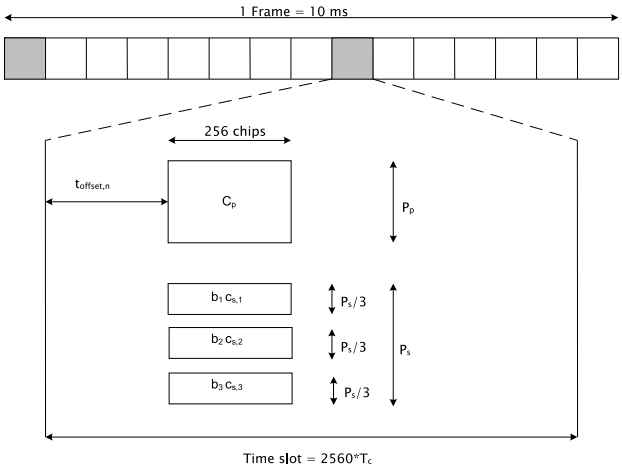

Figure 4. *Structure of the TDD synchronisation channel.*

stations from interfering. This will simplify our synchronisation task because once we have obtained synchronisation to the strongest base station (which can be done very reliably), we know where to look for the synchronisation channels of the other, weaker base stations.

Synchronisation Procedure. The synchronisation procedure proposed here uses one of the decision statistics $c(n)$ of Section II. As for the FDD mode, the peaks of $c(n)$ indicate the potential presence of a synchronisation code corresponding to a base station.

For primary synchronisation, the reference sequence $d(n)$ is the primary synchronisation code of length N. The result of primary synchronisation is the temporal position of the primary synchronisation code. For secondary synchronisation, $d(n)$ is the sum of the primary synchronisation code and three weighted secondary synchronisation codes. Since there exist 64 possible combinations of weighted secondary codes, we try all corresponding $d(n)$ and take the one yielding the largest value of $c(n)$ as the result of secondary synchronisation. Besides knowledge of the code group, this yields the time offset $t_{\text{offset},n}$ and with it the position of the slot border.

Synchronisation to the strongest base station. Primary and secondary synchronisation to the strongest base station are performed by taking the position of the highest peak in $c(n)$ as synchronisation timing. The result is quite reliable because the signal-to-noise-and-interference ratio (SNIR) of the strongest base station is high. Nevertheless, because the result of synchronisation to the strongest base station will heavily influence the synchronisation to the weaker base stations, we verify its correctness.

For this verification, we use the midamble sequence of the strongest base station as the reference sequence $d(n)$. We verify the presence of the midamble sequence at the expected location by checking if the peak of the detection statistic $c(n)$ obtained with the spatial detector (see Section II) is above a certain threshold. In the negative case, we repeat secondary synchronisation and midamble verification at the position of the second strongest peak of $c(n)$.

Synchronisation to the weaker base stations. After verifying the synchronisation to the strongest base station, we perform synchronisation to the weaker base stations. For this, we exploit the synchronicity property of TDD networks which consists in the temporal alignment of the slot borders of all base station signals.

The 32 possible time offsets $t_{\text{offset},n}$ of the synchronisation codes differ by multiples of 48 chips. Since base stations in adjacent cells never use the same time offset, we know where we can expect to find the synchronisation codes of weaker base stations. Because of path-length depending runtime differences, we search for the synchronisation codes in a certain time window around the expected locations, as shown in Fig. 5. The size of this window depends on the cell size and the expected maximal runtime differences. For synchronisation to a weaker base station, we accept a peak of $c(n)$ only if it *both* exceeds a certain threshold and is located within one of our time windows (see Fig. 5).

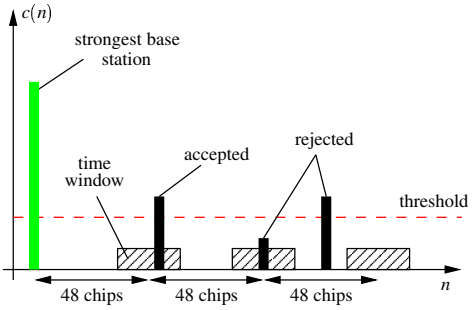

Figure 5. *Synchronisation to weaker base stations using time windows.*

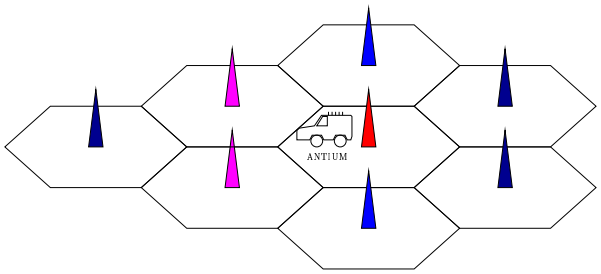

Figure 6. *Simulated network scenario.*

IV. SIMULATION RESULTS

For our simulations, we used Clarke's channel model [7] according to which the channel weight vector associated to the ith base station and the pth path is given as

$$\mathbf{h}_{i,p}(t) = \sum_{l=1}^{N_p^{(i)}} c_{p,l}^{(i)} \exp\left(\mathrm{j}\left[\frac{2\pi\nu}{\lambda\cos(\theta_{p,l}^{(i)}-\gamma)}t + \varphi_{p,l}^{(i)}\right]\right)\mathbf{s}_{p,l}^{(i)}.$$

Here, $N_p^{(i)}$ is the number of subpaths associated to the pth propagation path; $c_{p,l}^{(i)}$, $\theta_{p,l}^{(i)}$, $\varphi_{p,l}^{(i)}$, and $\mathbf{s}_{p,l}^{(i)}$ are respectively the attenuation, azimuth, phase, and steering vector of the lth subpath of the pth path; v is the speed of the mobile; γ is the angle between the mobile's motion and North; and λ is the wavelength. The angles $\varphi_{p,l}^{(i)}$ and γ are uniformly distributed.

The signal received from the nearest base station is corrupted by interference from the cells adjacent to the cell in which the mobile station is located. In our simulations, 7 interfering stations were taken into account (see Fig. 6). The control channel powers were fixed according to the standard [5]. The powers of the various base stations relative to the total received signal power are indicated in the first column of Tables 1–3.

We considered three different propagation environments, called "vehicular", "outdoor" and "indoor" in what follows, that differ by their cell radius and channel parameters. In addition, we used two different channel parameter settings (called A and B) for the outdoor and indoor environments. For the outdoor environment, channel A has three multipath components with a maximum delay of only 2 chips, whereas channel B has 8 taps with a maximum delay of 15 chips. For the indoor environment, channel A still has 3 taps with a maximum delay of 2 chips, but channel

Algorithm	Mono	Spatial	HST
Station 1: -1dB	100	100	100
Station 2: -11dB	24	100	100
Station 3: -11dB	56	100	100
Station 4: -18dB	0	42	75
Station 5: -18dB	0	29	79
Station 6: -22dB	0	1	5
Station 7: -22dB	0	10	25
Station 8: -22dB	0	7	34

Table 1. *Percentage of successful synchronisation events for UMTS FDD in the vehicular environment. The SNIR of the respective base station is shown in the first column. The columns labeled "Mono," "Spatial," and "HST" show the results obtained with the spatial detector using only a single antenna element, the spatial detector with 5 antenna elements, and the heuristic space-time detector (see Section II), respectively.*

B now has only 4 multipath components with a maximum delay of 3 chips. Since UMTS TDD is mainly designed for indoor and pedestrian applications, we used the indoor and outdoor environments for TDD and the vehicular environment for FDD.

A. *FDD Results*

In order to compare the performance of the spatial and space-time algorithms for the FDD mode, we generated 100 realisations of the received signal corresponding to the above described scenario using the vehicular propagation environment. The mobile velocity was 50 km/h. The performance of our algorithms is also compared to the classical mono-sensor algorithm that computes the temporal correlation between the received signal and the synchronisation sequence.

Table 1 indicates the percentage of successful synchronisation events for the vehicular environment vs. the SNIRs of the various base stations. We observe that the classical mono-sensor synchronisation algorithm always detects the main station and sometimes detects the two adjacent stations at -11 dB. The spatial synchronisation algorithm allows to detect all the stations with a relative power higher than -11 dB and sometimes allows to detect stations with a relative power of -18 dB. Below -18 dB, reliable detection is not possible anymore. Finally, the space-time synchronisation algorithm is superior to the spatial algorithm for the detection of stations at -18 dB, and it can sometimes detect stations down to -21 dB.

B. *TDD Results*

For the TDD mode, Table 2 shows the results for the outdoor environment with channel parameter configurations A and B. Table 3 shows analogous results for the indoor environment. In both cases, the mobile's velocity was set to 5 km/h.

These simulation results show that the spatial algorithm performs quite well, especially for channel A. Reliable synchronisation can be achieved down to an SNIR of about -15 dB for channel A and down to about -10 dB for channel B. For channel B, because of its larger delay, the space-time method shows superior performance, especially for the outdoor environment. Synchronisation using the space-time algorithm in the outdoor environment is possible down to about -18 dB for channel A and about -15 dB for channel B. For the indoor environment, the performance of the space-time algorithm for channel B is even slightly superior to that for channel A.

Algorithm	Mono		Spatial		HST	
Channel	A	B	A	B	A	B
Station 1: -1dB	100	99	100	98	100	99
Station 2: -11dB	37	17	100	92	100	99
Station 3: -11dB	35	23	100	90	100	99
Station 4: -18dB	8	0	91	20	97	64
Station 5: -18dB	7	0	94	26	97	61
Station 6: -22dB	1	1	59	2	61	12
Station 7: -22dB	1	0	59	3	67	23
Station 8: -22dB	1	0	78	6	78	33

Table 2. *Percentage of successful synchronisation events for UMTS TDD in the outdoor environment.*

Algorithm	Mono		Spatial		HST	
Channel	A	B	A	B	A	B
Station 1: -1.7dB	95	97	100	100	100	100
Station 2: -9.7dB	21	18	98	99	100	100
Station 3: -9.7dB	23	20	100	99	100	100
Station 4: -14.7dB	4	8	87	78	96	96
Station 5: -14.7dB	6	11	89	89	96	97
Station 6: -17.7dB	3	4	66	60	77	87
Station 7: -17.7dB	4	6	65	65	85	87
Station 8: -17.7dB	8	5	77	68	90	93

Table 3. *Percentage of successful synchronisation events for UMTS TDD in the indoor environment.*

V. CONCLUSION

In this paper, we compared the performance of two detection-based synchronisation algorithms in the context of the UMTS FDD and TDD downlinks. Roughly speaking, the spatial algorithm allows to detect base stations with SNIR about 7 dB lower than the mono-sensor algorithm. The space-time algorithm leads to an additional improvement of about 3 dB in comparison to the spatial algorithm.

The overall conclusion is that the use of multi-sensor algorithms allows to resolve interference situations that can seriously affect mobile reception.

REFERENCES

[1] P. Chevalier, F. Pipon, J. J. Monot, and C. Demeure, "Smart antenna for the GSM system: Experimental results for a mobile reception," in *Proc. IEEE Vehicular Technology Conference*, Phoenix, USA, May 1997, pp. 1572–1576.

[2] L. E. Brennan and I. S. Reed, "An adaptive array signal processing algorithm for communications," *IEEE Trans. Aerospace and Electronic Systems*, vol. 18, no. 1, pp. 124–130, Jan. 1982.

[3] D. M. Dlugos and R. A. Scholtz, "Acquisition of spread spectrum signals by an adaptive array," *IEEE Trans. Acoust., Speech, Signal Processing*, vol. 37, no. 8, pp. 1253–1270, Aug. 1989.

[4] Stephen M. Kay, *Fundamentals of Statistical Signal Processing: Detection Theory*, Prentice Hall, Upper Saddle River (NJ), 1998.

[5] 3GPP TS 25.211, "Physical channels and mapping of transport channels onto physical channels (FDD)," v. 3.2.0 (www.3gpp.org), March 2000.

[6] 3GPP TS 25.221, "Physical channels and mapping of transport channels onto physical channels (TDD)," v. 4.0.0 (www.3gpp.org), March 2001.

[7] R. H. Clarke, "A statistical theory of radiomobile reception," *Bell Syst. Tech. J.*, vol. 47, pp. 957–1000, 1968.